# The origins of friction and the growth of graphene, investigated at the atomic scale

Baarle, D.W. van

## Citation

Baarle, D. W. van. (2016, November 29). *The origins of friction and the growth of graphene, investigated at the atomic scale*. *Casimir PhD Series*. Retrieved from https://hdl.handle.net/1887/44539

**Author**: Baarle, D.W. van
**Title**: The origins of friction and the growth of graphene, investigated at the atomic scale
**Issue Date**: 2016-11-29

# Chapter 9

# Graphene film closure: strain and boundary defects

An important stage of the graphene synthesis process that has a significant impact on the final graphene quality is the closure of the graphene overlayer. In this stage, the individual, still growing graphene domains increasingly touch each other and connect. Depending on their relative alignment, neighbouring domains either merge or domain boundaries are formed between them. Those boundaries can influence the macroscopic properties of the graphene nanolayer, such as charge carrier mobility, yield strength, chemical inertness, etcetera[81, 82]. Here we report a study of graphene film closure, performed using our variable-temperature STM. An Ir(111) surface that was partially pre-covered with graphene was studied while the graphene film was closing. A clear preference of domains to connect to each other in ways that avoid the formation of local defects was observed. In case graphene domains were misaligned with respect to each other, they adjusted themselves by introducing internal deformation. This behaviour was observed through the deformation of the moiré patterns. For the first time, the build-up of strain in graphene was observed.

## 9.1 Observation of graphene film closure

The findings reported here are originating from two experiments in which we prepared the substrate slightly differently. The general procedure in both experiments was the same. The cleaned Ir(111) substrate was first pre-exposed to ethylene at room temperature. Then, the substrate was heated up in ultrahigh vacuum to a temperature at which practically all carbon had formed graphene. At this temperature, the surface was imaged by STM while it was further exposed to a low pressure of ethylene. The differences between the two experiments were the amount of ethylene the surface was pre-exposed to at room temperature (0.5 and 3 L) and the precise temperature at which the film-closure experiment was conducted (1067 and 1107 K respectively). Our experiments show that the precise temperature during the experiment did not seem to have a significant influence on the observations. The high-temperature exposure started at a partial pressure of ethylene of approximately $1 \times 10^{-10}$ mbar. As the graphene growth speed reduced over time, the ethylene pressure was slowly increased to approximately $7 \times 10^{-8}$ mbar. The temperature was not changed during the experiment and the gas exposure was stopped after the surface was entirely covered with graphene.

Three images extracted from the high-temperature STM observations are shown in Figure 9.1. These images were taken from Movie 2, which can be found in the electronic Supplementary Material. In these images, the orientations of two graphene domains are indicated by the dashed lines. The moiré patterns of the domains have a 4 ° difference in rotation angle with respect to each other. In combination with the observed lattice distances of the moiré patterns, we can conclude that the two graphene domains are rotated with respect to each other by 0.6 °. The two domains are positioned on two adjacent iridium terraces; one iridium step is situated in between the domains. It should be noted that, although the graphene domains look like depressions with respect to the iridium surface, they are actually situated on top of the iridium. The electronic structure of the Ir(111)/graphene system, in combination with the energy dependent LDOS of the STM tip and the applied sample bias voltage, reduces the tunnelling current via the graphene so much that it looks as if the graphene is positioned inside the iridium terraces rather than on top. A close look at other locations on the iridium surface and the application of several sample voltages revealed that the graphene was situated on top of the iridium surface.

The images in Figure 9.1 show how the two slightly misoriented graphene domains grow together to form one closed sheet of graphene. After the two domains have merged, no trace is left of the connection. Imperfections in the connection between the graphene lattices would have shown up in two ways, namely as noticeable imperfections in the moiré pattern and as strong ‘protrusions’ in the STM image due to the electronic structure of the local defects in the graphene lattice[83]. An example of a domain boundary that contains several defects is highlighted by the green arrow in Figure 9.1b.

A second observation that indicates that the graphene lattice does not

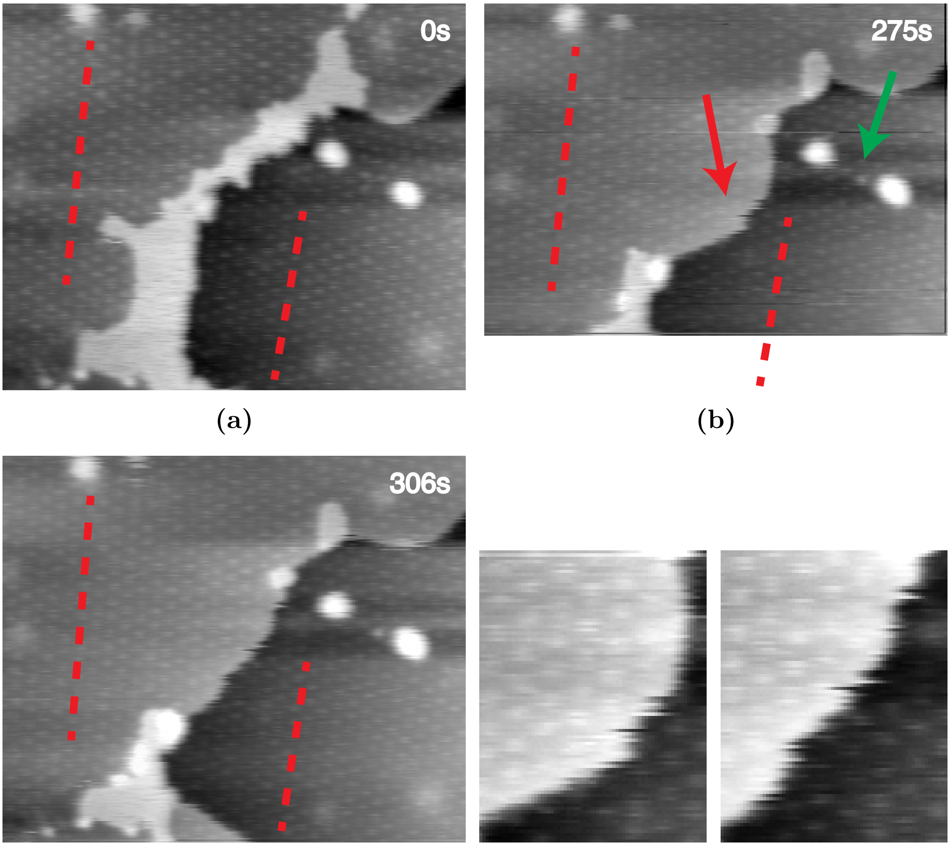

(a) (b)

(c) (d) (e)

**Figure 9.1:** (a)-(c) Three frames from an image sequence (frames 213, 219 and 220) in which the closure of the graphene overlayer on top of Ir(111) was followed by STM. The images were recorded at a temperature of 1067 K, while the surface was exposed to an ethylene partial pressure of $7 \times 10^{-8}$ mbar. The orientation of the moiré pattern in two graphene domains is highlighted by the dashed lines. The red arrow in panel (b) indicates the absence of a domain boundary between the two rotated graphene domains. The green arrow points at the domain boundary between two rotated graphene domains. The elapsed time is indicated in the top right corner of each image. Panels (d) and (e) are close-ups of the same area imaged in panels (b) and (c) and highlight the mobility of the iridium step underneath the graphene, also at the location where the two domains grew together. At the position of the seam between the domains (indicated by the red arrow), no domain boundary can be distinguished. Image size $73 \times 61\,\text{nm}^2$, z-scale 0.27 nm (for Figures (a)-(c)), sample voltage 3.1 V, tunnelling current 0.1 nA

contain defects along the line where the two domains merged, is that of the mobility of the iridium step underneath the graphene. This unhindered mobility suggests the absence of strong, local bonds from the overlayer to the iridium substrate. Such bonds would result in local pinning sites of the iridium to the graphene that reduce the mobility of the iridium surface layer locally. This effect is not observed. An additional advantage of the step mobility is that the line along which the graphene domains have merged, at or close to the step in the iridium substrate, can be inspected in several of the STM images with the step at some distance, thus enabling to view the seam without the complicating influence of the step.

When the orientations of two domains are sufficiently different, they can only connect by introducing a high-angle domain boundary that includes defects in the topology in the form of pentagons and heptagons[83]. The density of these defects along the domain boundary is dependent on the precise mismatch of the domains. An example of such a high-angle domain boundary with defects is indicated in Figure 9.1b by the green arrow.

## 9.2 Graphene domains locally align by strain

The only way for the differently oriented domains in Figure 9.1 to merge without the introduction of defects in the graphene topology is by tolerating changes in precise bond distances and bond angles, i.e. by introducing strain in the domains. The presence of such long-range deformations is illustrated clearly in Figure 9.2, which displays two STM images of graphene on Ir(111) recorded before and after film closure. For clarity, the individual graphene domains in the two images have been numbered. The temperature of this experiment was 1107 K, higher than that of the experiment of Figure 9.1, but this small difference is expected not to have significant impact on our findings.

The graphene sheet that is shown in Figure 9.2b exhibits moiré patterns that are clearly curved. When we look at the domains before film closure (Figure 9.2a) we can see that they all have different orientations. We find that when the domains come into contact with each other, not only defects are created at certain positions on the domain boundary, but also the graphene domains deform internally, such that the lattices match best with each other. This behaviour can be observed best by following the curving moiré patterns over multiple domains. The red lines in Figure 9.2c show how the internal distortions enable two domains to connect with a minimum of topology errors.

The curved moiré lattices indicate the presence of strain in the graphene.

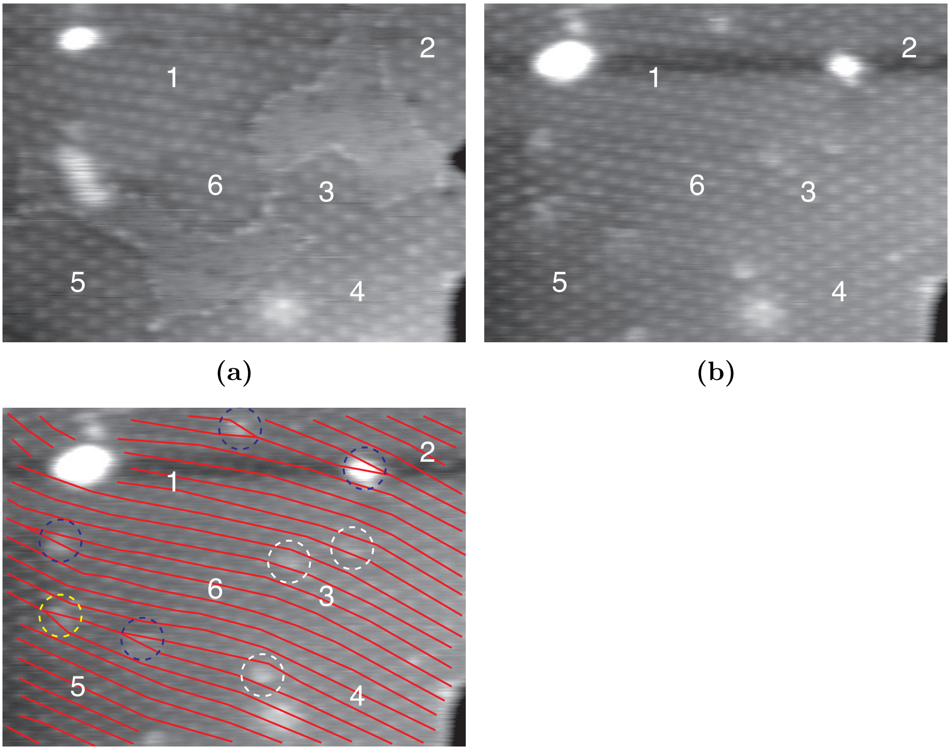

(a) (b)

(c)

**Figure 9.2:** (a) and (b) Two STM frames from a movie (frames 139 and 166) in which the closure of the graphene overlayer on Ir(111) was followed by STM. The images were recorded at temperatures of 1099 and 1107 K respectively, while a partial pressure of approximately $7 \times 10^{-8}$ mbar of ethylene was present. (c) Same image as shown in panel (b), with red lines connecting the maxima in the graphene domains across the image. Here, we have chosen one of the three principal directions of the moiré pattern. Similar sets of lines can be constructed along the other two. The dashed circles indicate point defects in the moiré pattern and are related to point defects in the graphene lattice, as discussed in the main text. Image size $59 \times 43\,\mathrm{nm}^2$, z-scale 0.16 nm, sample voltage 3.4 V, tunnelling current 0.1 nA, time between images: 780 sec.

A close look at the graphene deformation visible in Figures 9.2b and 9.2c shows that some lines are curved such that over a length of 5 moiré units, the lattice has curved over 1 moiré unit. The apparent shift of the moiré pattern over 1 unit means that the graphene lattice has deformed with an amount of 1 graphene lattice constant. Or, over a distance of $5 \times 10$ graphene lattice units, the graphene has deformed over 1 lattice unit. This means that a nominal strain of 0.02 was realized in the graphene bonds, which resulted in a deformation of approximately 0.003 nm of each carbon-carbon bond. These values are one order of magnitude lower than experimental and theoretical estimates of the maximum strain graphene can handle, which are in the range of $0.2 - 0.3$[84].

The build-up of strain in graphene costs energy. In case the amount of strain needed to align two domains, costs too much energy, the creation of local lattice defects will be more favourable than strain. These defects are observed in Figure 9.2b. The red lines in 9.2c make it easy to follow the moiré maxima over several domains along one of the three principal symmetry axes, and thus recognize the defects in the topology. Every defect, e.g. a pentagon-heptagon pair, in the graphene lattice leads to a single defect in the moiré pattern. In case two adjacent lines merge, a point defect appears. Each point defect is situated at a location where at least in two out of the three symmetry axes, lines merge. All defects are characterised by coloured, dashed circles. The colour of the circle denotes the kind of defect: the yellow colour means the defect shows up in all 3 symmetry directions (1 occurrence), the blue colour indicates the defect shows up in the symmetry direction highlighted by the red lines and another symmetry direction (4 occurrences). The white colour indicates that the defect shows up in the two other symmetry directions that are not highlighted by the red lines (3 occurrences). Our analysis has analogies with the work presented in Reference [83]. In that work, the defects that are labelled in our work by white and blue circles, are studied at the atomic scale. The defects are entitled as edge dislocations containing pentagon-heptagon carbon atom rings. This publication supports our findings. The only defect type that has not been reported before is the yellow-coded defect, which has impact on all three symmetry directions. We suggest that defect is actually a combination of two defects close to each other. As expected, point defects are inevitable in case domains with a significant misalignment merge.

## 9.3 Conclusions

Summarizing, we conclude that graphene domains growing together on iridium at high temperatures try to avoid the formation of defects in the form of domain boundaries. Most of the relative misalignment of the graphene domains is compensated by the introduction of long-range strain inside the graphene domains. Defects in the graphene lattice are known to influence the properties of graphene, such as the charge carrier mobility and other electronic properties[81, 85]. We expect that the introduction of strain instead of defects has much less impact on these properties, as the graphene lattice is not affected significantly. Also the mechanical strength and the chemical inertness of the graphene may be expected to be more favourable for the strained graphene than for defected graphene. Hence, the process of strain incorporation suppresses the impact of initially misaligned domains on the final quality of the graphene nanolayer.